Maximum separation between guide stars in atmospheric tomography

Venice 2001
Beyond Conventional Adaptive Optics

Andrei A. Tokovinin[a]

[a]Cerro Tololo Inter-American Observatory, Casilla 603, La Serena Chile

ABSTRACT

The quality of the tomographic wave-front reconstruction at large telescopes is limited by the vertical turbulence profile and by the configuration of guide stars (GSs). The tomographic error (in square radians) scales as $(\Theta r_0/\delta)^{5/3}$, where Θ is the size of GS constellation, r_0 is the Fried radius, and δ is the "effective thickness" of a given profile. Compared to the classical AO, the gain of the field-of-view size is proportional to the ratio of mean turbulence altitude $\bar{h}$ to δ, some ~ 10 times for real profiles with 3 GSs. It is shown that the residual anisoplanatism in a layer-oriented multi-conjugate adaptive optics system obeys a similar scaling law and that this approach offers a practically interesting sub-optimal solution of the tomographic problem. For a given total number of photons available from GSs, the photon noise in the compensated wave-front is proportional to the square of the number of layers. It means that even by increasing the number of layers it will not be possible to extend the correction into the visible range using only natural GSs, but laser GSs will be needed.

1. INTRODUCTION

The vertical soundings of atmospheric turbulence show that frequently the $C_n^2(h)$ profiles are dominated by few strong layers. It seemed logical that a better correction of turbulence would be achieved with several deformable mirrors (DMs), each conjugated to its own layer. In this vision of Multi-Conjugate Adaptive Optics (MCAO) (Dicke 1975, Beckers 1988) the number of DMs must equal the number of strong layers.

The phase screens corresponding to the individual layers should be measured separately. This is possible by means of *tomography* using the beams from several guide stars (GSs). Tallon & Foy (1990) have shown that, in order to solve for the unknown phase screens, the number of GSs must be no less than the number of corrected layers. Of course, the GS beams must overlap at the highest corrected layer, so the maximum separation between GSs is given by $\theta_{\rm beam} \sim D/H$, where H is the layer altitude and D is the telescope diameter.

With increasing telescope size, $\theta_{\rm beam}$ also increases, reaching 0.6° for $D = 100$ m and $H = 10$ km. In such a large field there will be enough natural guide stars (NGSs) for tomography, so laser guide stars (LGSs) may not be needed at all (Ragazzoni et al. 1999; Ragazzoni et al. 2000a). However, this reasoning completely ignores the turbulence between the strong layers. Even a small fraction of turbulence, if left uncorrected, would have a disastrous effect on the AO performance, especially for extremely large telescopes (ELTs). Let us recall that in a standard theory the atmospheric phase error scales as $(D/r_0)^{5/3}$. For example, leaving uncorrected only 1.5% of the total turbulence for a 100 m telescope would give the same error as for an 8 m telescope without adaptive optics, since $(8/100)^{5/3} = 0.015$.

Although the 5/3 scaling does not apply to very large apertures, it is clear that MCAO performance at ELTs must be evaluated carefully by taking into account *all* turbulence, not just few strong layers. It means that $\theta_{\rm beam}$ is not a relevant characteristic of the field-of-view (FOV) size, which in fact would be restricted by the shape of turbulence profile independently of telescope diameter. The whole evaluation of MCAO for ELTs needs to be re-considered from this point (Le Louarn et al. 2000). In this contribution we review the atmospheric FOV limits that apply to ELTs correcting turbulence with few DMs or using few GSs for tomography. We analyze the layer-oriented MCAO approach (Ragazzoni et al. 2000b) from this perspective.

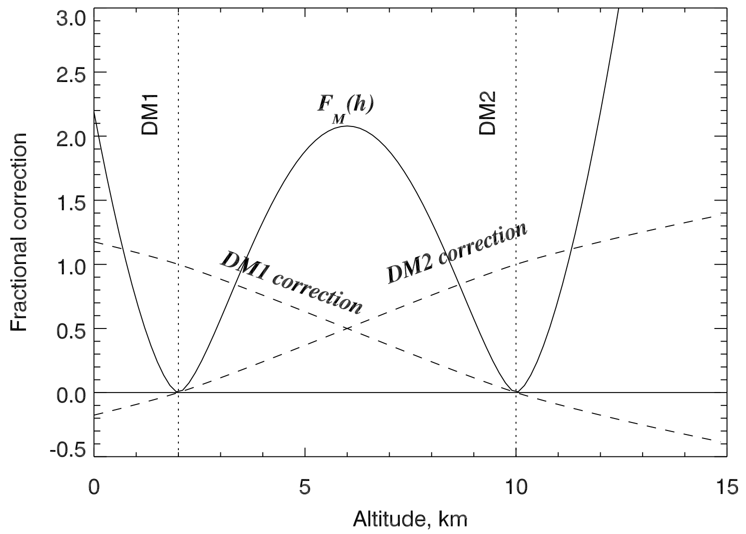

Figure 1. For two DMs conjugated to altitudes 2 and 10 km, the fractional corrections applied to each DM are plotted in dashed lines as a function of layer altitude (their sum equals 1). The full line shows $F_M(h)$ – a contribution of each layer to the residual anisoplanatism.

2. CORRECTION-LIMITED FOV

Let us assume that the instantaneous phase screens are known perfectly for all atmospheric layers, i.e. that we have reconstructed by some magic tool the 3-dimensional refractive index distribution. How large a field can be corrected with only few DMs?

This problem was addressed in (Tokovinin et al. 2000), here we provide a short summary. For each layer, the correction is distributed between all DMs in the proportions that minimize residual anisoplanatic errors (Fig. 1). Layers which do not coincide exactly with DMs contribute to the residual anisoplanatism with some weight $F_M(h, H_1, ..., H_M)$, where M is the number of DMs, $H_1, ..., H_M$ are their conjugation altitudes. Integrating over the altitudes, we obtain the residual phase error at a distance θ from the FOV center in the form

$$\langle \epsilon^2_{corr} \rangle = (\theta/\theta_M)^{5/3} \tag{1}$$

which is similar to Fried's expression relating the residual error to the classical isoplanatic patch size θ_0 (Fried 1982; Roddier 1999). Generalized isoplanatic angle θ_M is equal to a distance from the FOV center where the residual phase variance reaches 1 rad^2. It is defined as

$$\theta_M^{-5/3} = 2.905(2\pi/\lambda)^2 (\sec z)^{8/3} \int_0^{h_{max}} C_n^2(h) F_M(h, H_1, ..., H_M) \mathrm{d}h, \tag{2}$$

where $C_n^2(h)$ is the profile of the refractive index structural constant, z is the source zenith angle, λ is the imaging wavelength. The recipe for calculating F_M is provided in (Tokovinin et al. 2000).

Now the optimum conjugation altitudes can be found for each particular turbulence profile by maximizing θ_M. This maximum θ_M is system-independent, being only a function of the $C_n^2(h)$ profile, the wavelength, and the number of DMs. The calculations for some real profiles are given in (Le Louarn et al. 2000; Tokovinin et al. 2000). With 2 DMs, one gains in the FOV size by 4–5 times, with 3 DMs – 7–10 times with respect to the classical isoplanatic patch θ_0. For a large M the gain θ_M/θ_0 becomes proportional to M.

Distributing a correction of each phase screen proportionally between the DMs is not the best available strategy: lower errors can be obtained if some high-frequency part of the turbulence spectrum is removed from the correction. This additional optimization depends on the desired FOV. However, the improvement over proportional control is not dramatic, hence θ_M is a good first-order estimate of the correction-limited FOV.

With a typical isoplanatic patch size of $\theta_0 = 2''$ (at $\lambda = 0.5$ μm), the 3-DM system would have a FOV radius of only $\sim 20''$ – *much* less than the geometrical limit $\theta_{\rm beam}$ quoted above. Even in the K band ($\lambda = 2.2$ μm), where the isoplanatic FOV is 5.9 times wider, the MCAO field at ELTs will be limited by the residual anisoplanatism and not by beam overlap.

Further author information: E-mail: atokovinin@ctio.noao.edu

3. TOMOGRAPHY-LIMITED FOV

In the previous section we supposed the instantaneous perturbations in all layers to be known, although in reality they must be deduced from the signals of wave-front sensors (WFSs), each of them observing its own GS. The number of reconstructed layers must not exceed the number of GSs, which means that with few GSs it is not possible to do a full tomography of the whole turbulent volume. Instead, a best possible estimate of a wave-front correction for some scientific target can be constructed from the signals of off-axis GSs. We employ the term *tomography* in this sense, like Ragazzoni et al. (2000a) who demonstrated it in a real experiment. Evidently, tomography can be used to correct the image of a faint scientific target even with one DM, provided that suitably bright GSs can be found in a wider field. How wide this field can be?

In the context of ELTs, wave-fronts may be considered to be of infinite size, which permits to apply the Fourier technique to this problem. At each spatial frequency, the components of target wave front are found as a linear combination of the GS signals. When the WFS noise is taken into account and an estimate with minimum residual error is sought, something resembling a Wiener filter is obtained; the details can be found in (Tokovinin & Viard 2001). Neglecting the WFS noise, the atmospheric component of the tomographic error $\langle \epsilon_{tom}^2 \rangle$ can again be represented in the familiar form,

$$\langle \epsilon_{tom}^2 \rangle = (\Theta/\gamma_K)^{5/3}, \tag{3}$$

where Θ is the radius of a constellation of K GSs and γ_K is the tomographic patch size. This apparently simple formula hides the inherent complexity of the problem (for example, $\langle \epsilon_{tom}^2 \rangle$ depends on the viewing direction; different definitions of Θ lead to different values of γ_K). However, the 5/3 scaling with Θ always holds, as well as the dependence of γ_K on the wavelength, expressed through the Fried radius r_0 as

$$\gamma_K = r_0/\delta_K. \tag{4}$$

The parameter δ_K may be regarded as some "equivalent thickness" of a turbulent profile. The widening of tomographic FOV compared to normal isoplanatic patch is simply $\bar{h}/\delta$. Here $\bar{h}$ is the mean turbulence altitude, $\theta_0 = r_0/\bar{h}$ (Roddier 1999). Although the height of the standard atmosphere is only 8 km and most of the turbulence is concentrated in the lower layers, the $h^{5/3}$ weighting in the calculation of $\bar{h}$ leads to characteristic values of $\bar{h} \approx 10$ km.

For typical real profiles and symmetric configurations of guide stars, $\delta_3 \approx 1$ km and $\delta_5 \approx 0.5$ km. It means that the FOV gain of tomography vs. classical AO is 10 to 20 times. Hence, the atmospheric limit on the size of GS constellation is somewhat less strict than the correction limit discussed above. However, here we compare two different things: θ_M describes the increase of the residual error with increasing distance from the FOV center, while γ_K describes the residual error at the very center of the FOV which results from the size of GS constellation.

For profiles consisting of N thin discrete layers, $\delta_K = 0$ if $K \geq N$. In this case the layers (hence *all* turbulent volume) can be reconstructed precisely and the FOV will be ultimately limited by $\theta_{\rm beam}$. Unfortunately, this situation is only of academic interest.

4. LAYER-ORIENTED SYSTEMS

Following the idea of Beckers (1988), Ragazzoni et al. (2000b) proposed to sense the wave-fronts not at the telescope pupil but in the planes conjugated to DMs. It makes no difference as long as each GS is sensed separately, but if the signals of all GSs could be mixed together (averaged), the contribution of the sensed layer would be preserved, while the contributions of other layers would be smeared and diminished. Such "averaged" WFS can control the corresponding DM directly. The *layer-oriented* approach consists in using an independent closed-loop compensation for each layer, so that the whole MCAO system will consist of several DM-WFS pairs, each one conjugated to a different altitude. It is argued that such a system may be less complex and less demanding in terms of real-time computer speed. An additional advantage of a layer-oriented system (LOS) may consist in a better use of the light from many faint NGSs and in some sensitivity benefits from tracking the wind-driven turbulence in individual layers with a longer exposure time (Ragazzoni et al. 2000b).

It is evident that there will be some cross-talk between the layers. As shown in Fig. 2, a point P_1 at the first layer conjugated to an altitude H_1 will sense the turbulence in this layer directly, but some other layer at

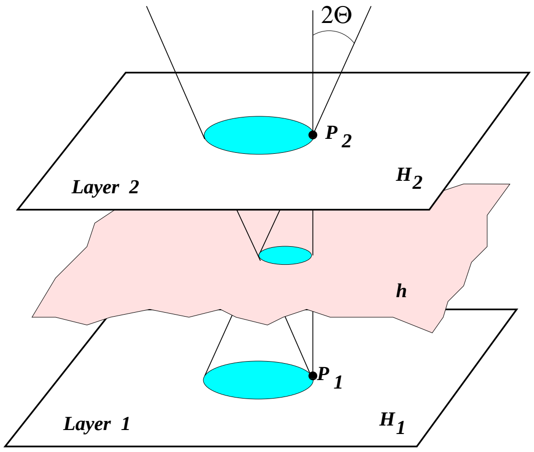

Figure 2. Layer-oriented MCAO system. The turbulence at a point P_1 in layer 1 is measured directly, but a contribution from another layer at an altitude h is smoothed proportionally to the diameter of guide star constellation 2Θ. Similarly, layer 2 "sees" its own turbulence directly, while other layers are smoothed.

an altitude h will be smoothed at a spatial scale of $2\Theta(h - H_1)$, where Θ is the radius of the GS constellation. A phase correction applied to layer 2 will be sensed at layer 1 with a smoothing length of $2\Theta(H_2 - H_1)$. It is expected that in a closed loop operation the system will be able to disentangle the layers and to "solve" the tomographic problem in hardware, not needing a powerful computer.

The closed-loop operation of a LOS is described in Appendix A in the quantitative way, assuming that each layer can measure and compensate turbulence with infinite spatial resolution and that the layers have infinite extent (a good approximation for ELTs). Again, the Fourier approach is exploited. This treatment permits to compute the residual anisoplanatism in a similar manner as in previous sections. The noise propagation in a LOS is also assessed.

4.1. Tomographic error in LOS

A LOS can be viewed as a specific case of turbulence tomography, solving for 3-dimensional phase perturbations from the signals of several GSs. It is instructive to compute the resulting tomographic error, neglecting for the moment the WFS noise. As shown in the Appendix, the tomographic error $\langle \epsilon^2_{\rm tom} \rangle$ is equal to

$$\langle \epsilon^2_{\rm tom} \rangle = \Theta^{5/3} \int {\rm d}h C_n^2(h) F_L(h, H_1, ..., H_L) = (\Theta/\theta_L)^{5/3}, \tag{5}$$

$$F_L(h, H_1, ..., H_L) = 9.69 \cdot 10^{-3} (2\pi)^3 \lambda^{-2} \int_0^\infty {\rm d}f' f'^{-8/3} |G(f')|^2. \tag{6}$$

Here L is the number of layers, H_L are the layer conjugation altitudes, Θ is the radius of GS constellation, $|G(f')|^2$ is the averaged in angle squared modulus of the error transfer function (16). The conjugation altitudes can be adjusted to minimize $\langle \epsilon^2_{\rm tom} \rangle$ for a given turbulence profile. A parameter θ_L is the radius of GS configuration in a LOS which corresponds to a 1 rad^2 wave-front error at a given wavelength (at the center of FOV). This patch size is computed from Eqs. 5, 6. It depends on the turbulence profile, the number of GSs, and layer conjugation altitudes, and is proportional to $\lambda^{6/5}$ as many other atmospheric parameters. Below we explore two extreme GS configurations: 3 GSs at a distance Θ from the FOV center and a continuous distribution of many GSs in a circle of radius Θ. Comparing many- and few-GS configurations gives an idea of the influence of GS number in LOS systems.

In Fig. 3 the functions $F_L(h)$ which give the relative contribution of layers to the residual anisoplanatism are plotted for those two cases. Both go to zero at layer conjugation altitudes and have a maximum between the layers. However, for many GSs the weights are ~ 10 times smaller, leading to isoplanatic patch size ~ 3 times larger. The shape of these functions is qualitatively similar to the shape of correction-limited altitude weighting $F_M(h)$ which is also plotted in Fig. 3 for the same 2-layer configuration.

In Fig. 4 the dependence of the isoplanatic patch size θ_L on the conjugation altitude of the second layer is shown for a 7-layer Cerro Pachon turbulence model given in (Ellerbroek & Rigaut 2000) and based on numerous profile soundings (Vernin et al. 2000). As expected, θ_L is smaller in the 3-GS case. The smoothness of $F_L(h)$ translates into the shallow dependence of the isoplanatic patch on the conjugation altitude, clearly seen in Fig. 4. Unless there are really strong layers in the atmosphere, the exact conjugation altitude of the upper DM/WFS combination is not very critical.

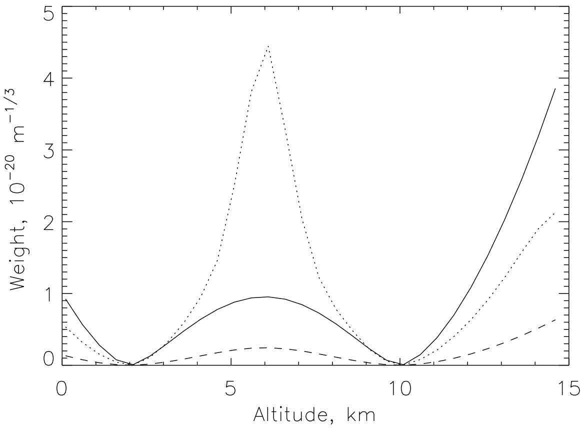

Figure 3. The residual anisoplanatism weighting functions $F_L(h)$ for a LOS with 2 layers conjugated to 2 and 10 km. Dotted line shows the case of 3 GSs, dashed line - a weighting function for many GSs. The $F_M(h)$ for correction-limited anisoplanatism is overplotted in full line for comparison.

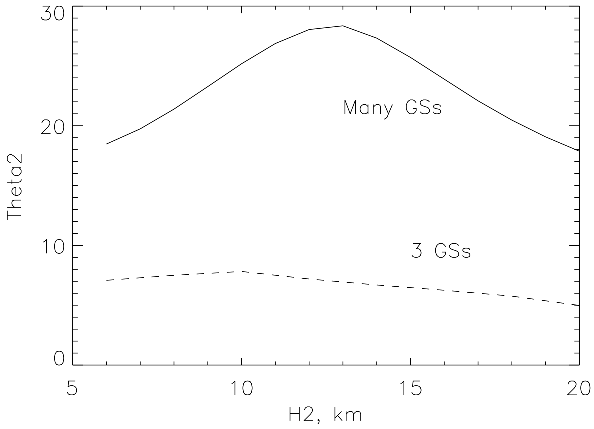

Figure 4. Isoplanatic patch size θ_2 (in arc-seconds, $\lambda = 0.5$ μm) for a 2-layer system as a function of the conjugation altitude H_2 ($H_1 = 0$) for the Cerro Pachon 7-layer model. The many-GS case is traced in full line, 3-GS case – in dashed line.

As a next step, we take the 12 turbulence profiles measured at Cerro Paranal during the PARSCA campaign (Fuchs & Vernin 1996) and compute the patch sizes for 3-GS and many-GS cases with two layers conjugated to 0 and 10 km. Note that somewhat larger angles would be obtained if the conjugation altitudes were optimized individually for each profile. Still, the patch size (at 0.5 microns) is quite large. Moreover, there is an approximate proportionality between the classical isoplanatic patch size θ_0 and θ_L, with coefficients 3 and 10 for the 3-GS and many-GS cases (Fig. 5). Despite the widely different shapes of individual profiles, the patch size behaves in almost predictable manner!

It might seem suspicious that a 2-layer LOS can have a FOV larger that the correction-limited MCAO with 2 DMs ($\sim 10\theta_0$ and $\sim 5\theta_0$, respectively). How can a 2-layer LOS outperform the 2-DM MCAO with *perfectly known* turbulence and optimized corrections? In fact it does not, because we compare two different things, the on-axis tomographic error with the off-axis correction error. Comparing LOS with tomography (Sect. 3), we see that with 3 GSs the allowable size of GS constellation is ~ 3 times smaller for LOS ($3\theta_0$ and $10\theta_0$, respectively). Thus, LOS performs worse, but not dramatically worse, given the fact that it is an analogue system not using any apriori information on turbulence spatial spectrum, $C_n^2(h)$ profile, etc. LOS is a practically interesting sub-optimal solution of the tomographic problem.

4.2. Noise propagation

The noise propagation factor Q (Eq. 19) depends on the number of layers and on their conjugation altitudes. When the matrix A is well-conditioned (which means that the layers are well de-coupled), the elements of A^{-1} and hence Q have reasonably small values. This happens at high spatial frequencies. However, even if A is the identity matrix, $Q = L$. In a LOS the overall noise is proportional to the number of layers, which is not surprising given that all layers contribute to the residual phase error.

At spatial frequencies lower than $f_0 = (2\Theta d)^{-1}$, where d is a typical distance between the layers, there is a significant cross-talk, leading to large A^{-1} and large Q. The low-frequency information supplied by the WFSs is almost identical and hence insufficient to solve the tomographic problem. However, such a solution is not needed, because low frequencies can be well corrected with only one layer.

In calculating the noise propagation factor Q plotted in Fig. 6, we used Singular Value Decomposition (SVD) for inversion of A, rejecting the eigenmodes with low singular values. They are rejected only at low frequencies, automatically reducing the effective number of controlled layers. Of course, the noise propagation is also reduced and at the lowest frequencies tends to L^{-1}. It means that the signals of all L WFSs are averaged and used to control a single layer. However, we do not know if something similar to SVD filtering can actually be implemented in an analogue system like LOS.

In a 2-layer LOS at low frequencies the elements of A^{-1} are large but of opposite sign, happily canceling out in Eq. 17. So, even without additional tricks Q stays low; this does not hold for 3 and more layers.

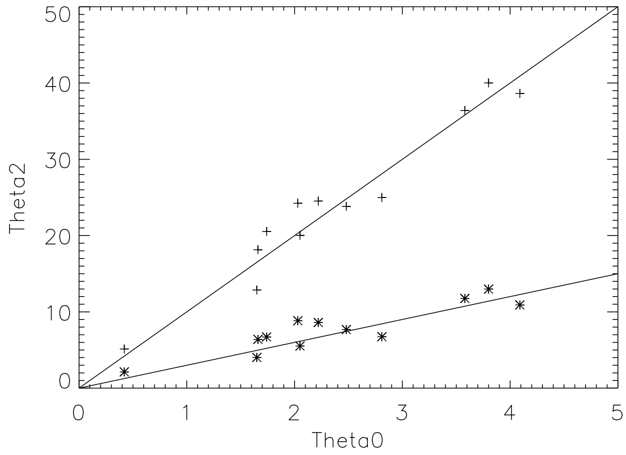

Figure 5. Isoplanatic angle θ_L (arc-seconds, $\lambda = 0.5$ μm) for the many-GS (crosses) and 3-GS (asterisks) cases against θ_0 for 12 turbulence profiles at Cerro Paranal. Two layers are conjugated to 0 and 10 km. The lines shows approximate proportionality between the angles with coefficients 10 and 3.

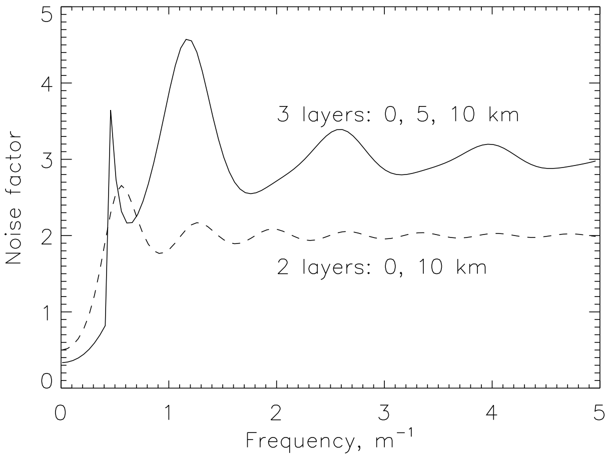

Figure 6. The noise propagation factor $Q(f)$ for a 2- and 3-layer LOS (dashed and full lines) with many GSs in a FOV of $30''$ radius ($f_0 \approx 0.7$ m^{-1}).

Supposing that the problem of low-frequency noise is somehow solved, the overall WFS noise will be dominated by the contribution of high frequencies. With a total of N photons available from all GSs for L layers, each layer will receive $n = N/L$ photons. It is known that noise variance of the reconstructed phase is proportional to n^{-1}. Taking into account that $Q \approx L$, we arrive to a conclusion that in a layer-oriented system *error due to WFS noise is proportional to* L^2.

5. SCALING MCAO TO THE VISIBLE

The difficulty of pushing the AO correction into the visible range is well known. The main problem lies in getting a sufficient number of photons to measure wave-fronts. Both the spatial scale of correction and the coherence time are proportional to $\lambda^{1.2}$, which means that the required photon flux must increase as $\lambda^{-3.6}$ when going to shorter wavelengths.

MCAO opens up the corrected field and holds a promise to get more photons from natural GSs. Unfortunately, as we have seen, the gain in the FOV size over traditional AO is limited by the residual anisoplanatism to a factor ranging from 5 to 10 for MCAO systems with small number of DMs and GSs. Under favorable atmospheric conditions the diameter of corrected FOV can perhaps reach 1 arc-minute at a wavelength of 0.5 μm (or $\sim 6'$ in the K band). It is clear that finding 3 NGSs of magnitude 9-10 in a $1'$ FOV is so rare that a simple MCAO system with NGSs would have a negligible sky coverage at optical wavelengths.

Can we mitigate this limitation by increasing the number of corrected layers? For large L, the size of corrected FOV will increase in proportion to L. The total flux of NGSs in this field will be proportional to L^2. Even if we can use all this flux efficiently in a layer-oriented MCAO system, the noise propagation factor $Q \propto L^2$ cancels the gain, and the residual phase error is no less than in an MCAO with smaller number of layers. For a "classical" optimized MCAO system (one WFS per each GS) noise propagation was treated in (Tokovinin & Viard 2001). There is no simple formula, but photon noise does increase with increasing GS separation.

Our conclusion is that even with a very large number of corrected layers there will be not enough photons from natural stars to push the correction into the visible range. The perspective of doing MCAO in the visible is entirely dependent on artificial laser GSs.

6. CONCLUSIONS

Although turbulence tomography and MCAO can increase the corrected FOV of adaptive systems with respect to classical AO, this gain remains modest, of the order of 5–10 for first-generation systems, because atmospheric anisoplanatism is reduced but not removed completely. Hence, early estimates of FOV size based only on the beam overlap turned out to be too optimistic.

We analyze the residual anisoplanatism and noise propagation in a layer-oriented MCAO system and show that this approach may offer a practically interesting hardware solution to the turbulence tomography problem. Still, carefully optimized MCAO systems which use additional information on turbulence profile and noise will likely out-perform layer-oriented systems.

For a very large number of layers, the increased number of photons available from the NGSs in a wider FOV does not lead to reduced errors of compensated wave-fronts because the noise propagation cancels this gain. Hence, the perspective of AO correction in the visible range is related to laser GSs.

APPENDIX A. THEORY OF LAYER-ORIENTED SYSTEMS

WFS signal in LOS. At first, we determine the reaction of LOS to a single turbulent layer at an altitude h which produces a phase perturbation $\phi(\vec{x})$ (Fig. 2), where $\vec{x}$ is a coordinate in the plane of layer.

Let us suppose that there are K GSs in the FOV, characterized by their positions $\vec{\theta}_k$ and by their intensities s_k. A WFS which is conjugated to an altitude H_l averages the phase screens from all GSs with the weights proportional to s_k and with the spatial shifts $\vec{\theta}_k(h - H_l)$ (as usual, the hypothesis of weak perturbations and the geometric-optics approximation are adopted here). A *smoothing function* $W_\theta(\vec{x}, d)$ describes the spatial averaging of a wave-front at a distance d from the layer:

$$W_\theta(\vec{x}, d) = \left(\sum_k s_k \right)^{-1} \sum_k s_k \; \delta(\vec{x} - d\vec{\theta}_k), \tag{7}$$

where $\delta(\vec{x})$ is a Dirac's delta-function. Thus, the WFS signal $\Delta_l(\vec{x})$ produced by a single layer is a convolution:

$$\Delta_l(\vec{x}) = \phi(\vec{x}) \odot W_\theta(\vec{x}, h - H_l). \tag{8}$$

In addition to the atmospheric perturbation ϕ the WFS will "see" the correction signals $\psi_j(\vec{x})$ applied to all layers, also convolved with W_θ (Eq. 8 would be valid only for zero corrections). We also take into account the WFS noise $\nu_l(\vec{x})$, hence the complete *error signal* $\Delta_l(\vec{x})$ for a layer l becomes

$$\Delta_l(\vec{x}) = \phi(\vec{x}) \odot W_\theta(\vec{x}, h - H_l) - \sum_{j=1}^{L} \psi_j(\vec{x}) \odot W_\theta(\vec{x}, H_j - H_l) + \nu_l(\vec{x}). \tag{9}$$

Now we pass from coordinates $\vec{x}$ to spatial frequencies $\vec{f}$, denoting the Fourier transforms (FT) by tilde. The convolutions turn into products. Considering the error signals, corrections, and noise in all L layers as vectors $\tilde{\Delta}$, $\tilde{\psi}$, $\tilde{\nu}$ of a length L, we re-cast Eq. 9 in a compact matrix form as

$$\tilde{\Delta}_l = \tilde{\phi} B - A\tilde{\psi} + \tilde{\nu}. \tag{10}$$

The matrix A and the vector B are

$$a_{ij} = \tilde{W}_\theta[\vec{f}(H_j - H_i)], \quad b_i = \tilde{W}_\theta[\vec{f}(h - H_i)]. \tag{11}$$

Note that d enters only as a product $d\vec{f}$ in the FT of the smoothing function.

$$\tilde{W}_\theta(d\vec{f}) = \left(\sum_k s_k \right)^{-1} \sum_k s_k \; \exp[-2\pi i d(\vec{f} \cdot \vec{\theta}_k)]. \tag{12}$$

In the most favorable case when a very large number of GSs is observed, filling uniformly a circular FOV of radius Θ, the smoothing function can be approximated by a circle. Its FT is related to Bessel function J_1:

$$\tilde{W}_\theta(d\vec{f}) = \frac{J_1(2\pi\Theta|\vec{f}|d)}{\pi\Theta|\vec{f}|d}. \tag{13}$$

Closed-loop operation of LOS. The servo system tries to drive the error signals to zero. Supposing that it is fast enough to follow the atmospheric changes and that DMs have unlimited spatial resolution, the correction signal $\tilde{\psi}$ can be found from the solution of the linear system $\tilde{\Delta} = 0$. It follows from Eq. 10 that

$$\tilde{\psi} = A^{-1}(\tilde{\phi} B + \tilde{\nu}). \tag{14}$$

Once the correction signals are known, we can compute the residual error of the compensated wave-front $\tilde{\epsilon}$. For an on-axis target, it equals the perturbation minus all corrections:

$$\tilde{\epsilon} = \tilde{\phi} - \sum_{l=1}^{L} \tilde{\psi}_l = G(\vec{f})\tilde{\phi} + C^T \tilde{\nu}, \tag{15}$$

where

$$G(\vec{f}) = 1 - \sum_{i=1}^{L}\sum_{j=1}^{L} (a^{-1})_{ij} b_j = 1 - \mathbf{1}^T (A^{-1}B), \tag{16}$$

$$c_i = - \sum_{j=1}^{L} (a^{-1})_{ji} \ \text{ or } \ C = \mathbf{1}^T A^{-1}. \tag{17}$$

The superscript ^{T} means matrix transpose, $\mathbf{1}$ stands for a column vector of the length L with unit elements. The *error transfer function* $G(\vec{f})$ defines the part of the turbulence spectrum which remains uncorrected. It grows from 0 at small $|\vec{f}|$ to 1 at $|\vec{f}| >> f_0$, where a characteristic frequency $f_0 = (2\Theta d)^{-1}$ depends on the constellation size Θ and distance between the layers d. At low frequencies the growth is quadratic. For a 2-layer system, the error transfer function is

$$G(\vec{f}) = \frac{1 + \tilde{W}_\theta[\vec{f}(H_2 - H_1)] - \tilde{W}_\theta[\vec{f}(h - H_1) - \tilde{W}_\theta[\vec{f}(h - H_2)]}{1 + \tilde{W}_\theta[\vec{f}(H_2 - H_1)]}. \tag{18}$$

Residual variance. The power spectrum of the residual phase error $\langle|\tilde{\epsilon}(\vec{f})|^2\rangle$ now may be related to the power spectrum of atmospheric perturbations $\langle|\tilde{\phi}(\vec{f})|^2\rangle = \Phi_\phi(\vec{f}, h)$ and to the noise power spectra $\nu_l^2(\vec{f})$. For simplicity we suppose that WFS noise spectrum is identical in all layers, $\nu_l^2(\vec{f}) = \nu^2(\vec{f})$ (all WFSs use the same light, which is assumed to be divided in equal proportions between the layers). Thus, a *noise propagation factor* Q can be defined as

$$Q(\vec{f}) = \sum_{i=1}^{L} |c_i|^2. \tag{19}$$

Now the power spectrum of phase residuals is written as

$$\langle|\tilde{\epsilon}(\vec{f})|^2\rangle = \Phi_\phi(\vec{f}, h)\ |G(\vec{f}, h)|^2 + Q(\vec{f})\ \nu^2(\vec{f}). \tag{20}$$

The atmospheric phase spectrum for a layer at altitude h and a wavelength λ (Kolmogorov spectrum, e.g. Roddier 1999) is related to the refractive index structure constant $C_n^2(h)$:

$$\Phi_\phi(\vec{f}, h) = 9.69 \cdot 10^{-3} (2\pi/\lambda)^2 |\vec{f}|^{-11/3} C_n^2(h) \mathrm{d}h. \tag{21}$$

Summing up the contributions of all atmospheric layers (which are statistically independent) and integrating the power spectrum over spatial frequencies $\vec{f}$, we finally obtain the total residual variance $\langle\epsilon^2\rangle$:

$$\langle\epsilon^2\rangle = \int \mathrm{d}h \int \mathrm{d}\vec{f}\ \Phi_\phi(\vec{f}, h)|G(\vec{f}, h)|^2 + \int \mathrm{d}\vec{f}\ Q(\vec{f})\ \nu^2(\vec{f}). \tag{22}$$

The dependence of the tomographic error $\langle\epsilon^2_{\rm tom}\rangle$ (the first term of the Eq. 22) on the size of GS constellation Θ can be singled out by the change of variables $\vec{f'} = \Theta\vec{f}$ and $\vec{\theta'} = \vec{\theta}/\Theta$. This transformation does not change the W_θ and hence A, B, and G, because they depend only on the scalar products $(\vec{f}\cdot\vec{\theta})$. In Eq. 21 $\Theta^{11/3}$ appears after change of variables, converted to $\Theta^{5/3}$ after double integration over $\vec{f'}$. The atmospheric spectrum depends only on the modulus of the spatial frequency $f = |\vec{f}|$. The same is true for $|G(\vec{f})|^2$ in case of uniformly distributed GSs (for sparse GS configurations, we denote by $|G(f)|^2$ the two-dimensional filter $|G(\vec{f})|^2$ averaged in angle). This permits to express $\langle\epsilon^2_{\rm tom}\rangle$ by Eqs. 5,6.

REFERENCES

Beckers J. M., "Increasing the size of the isoplanatic patch with multiconjugate adaptive optics", in *Proc. ESO Conf. on Very Large Telescopes and their Instrumentation,* M.-H. Ulrich, ed., pp. 693-703, ESO, Garching bei München, 1988.

Dicke R. H., "Phase-contrast detection of telescope seeing errors and their correction," *Astrophys. J.* **198**, pp. 605-615, 1975.

Ellerbroek B. L. and Rigaut F., "Scaling multiconjugate adaptive optics performance estimates to extremely large telescopes," in *Adaptive Optical Systems Technology",* P. L. Wizinovich, ed., *Proc. SPIE*, **4007,** pp. 1088-1099, 2000.

Fried D.L., "Anisoplanatism in adaptive optics," *J. Opt. Soc. Amer. A*, **72**, pp. 52-61, 1982.

Fuchs A. and Vernin J. "Final Report on PARSCA 1992 and 1993 campaigns," *ESO Report VLT-TRE-UNI-17400-0001*, ESO, Garching bei München, 1996.

Le Louarn M., Hubin N., Sarazin M., and Tokovinin A., "New challenges for Adaptive Optics: Extremely Large Telescopes", *Mon. Notices Roy. Astron. Soc.*, **317,** pp. 535-544, 2000.

Ragazzoni R., "No laser guide stars for adaptive optics in giant telescopes?", *Astron. Astrophys. Suppl. Ser.*, **136**, p. 205-209, 1999.

Ragazzoni R., Marchetti E., and Valente G., "Adaptive-optics corrections available for the whole sky," *Nature*, **403**, p. 54-56, 2000.

Ragazzoni R., Farinato J., and Marchetti E., "Adaptive optics for 100m class telescopes: new challenges require new solutions," in: *Adaptive Optical Systems Technology,* P. L. Wizinovich, ed., *Proc. SPIE*, **4007,** pp. 1076-1087, 2000.

Roddier F, ed., *Adaptive optics in astronomy*, Cambridge Univ. Press, Cambridge, 1999.

Tallon M. and Foy R., *Astron. Astrophys.*, **235**, p. 549-557, 1990.

Tokovinin A., Le Louarn M., and Sarazin M., "Isoplanatism in a multi-conjugate adaptive optics system," *J. Opt. Soc. Amer. A.*, **A17**, pp. 1819-1827, 2000.

Tokovinin A. and Viard E., "Limiting precision of tomographic phase estimation," *J. Opt. Soc. Amer. A.*, **A18**, pp. 873-882, 2001.

Vernin J., Agabi A., Avila R., Azouit M., Conan R., Martin F., Masciadri E., Sanchez L., and Ziad A., "Gemini site testing campaign. Cerro Pachon and Cerro Tololo," *Gemini RPT-AO-G0094, http://www.gemini.edu/*, 2000.